Macromolecules

Article

pubs.acs.org/Macromolecules

Facile Syntheses of Cucurbit[6]uril-Anchored Polymers and Their Noncovalent Modification

Xiaoling Huang, Fanglin Hu, and Haiquan Su*

School of Chemistry and Chemical Engineering, Inner Mongolia University, Hohhot, 010021, China

Supporting Information

ABSTRACT: The general strategy for facile synthesis of Cucurbit[6]uril- (CB[6]-) anchored polymers without the functionalization of CB[6] was presented. The acrylamide as a typical monomer was used to synthesize a series of CB[6]-anchored polyacrylamides (CB[6]-PAM) using potassium persulfateas as initiator and oxidant. The CB[6]-PAM samples were characterized by ^{1}H NMR, ^{13}C NMR, HMQC, FTIR, and TGA. It was found that the composition and chain microstructure of CB[6]-PAM polymers could be tunable by changing the content of potassium persulfate, CB[6] and acrylamide. In addition, CB[6]-PAM could be assembled into nanosized vesicles, which were confirmed by TEM, AFM, and SEM measurements. By taking advantage of the exceptional binding affinity of the CB[6], the CB[6]-PAM could be modified with butyl amine hydrochloride. The result makes the CB[6]-anchored polymer potentially useful in many applications. Furthermore, this synthetic approach could be extend to CB[6]-anchored polymers with two different chains. As a typical example, CB[6]-anchored poly(4-vinylbenzylamine hydrochloride salt) and polyacrylamide was synthesized successfully.

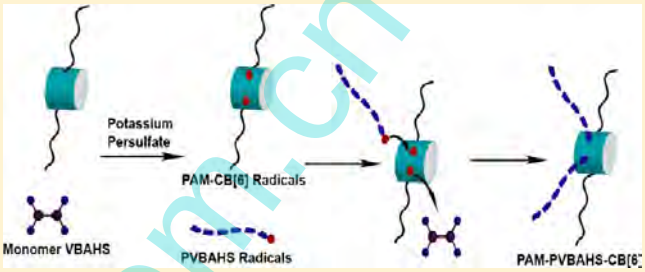

INTRODUCTION

Cucurbit[6]uril, a macrocyclic cavitand comprised of six glycoluril units, has a hydrophobic cavity of 5.5 Å diameter that is accessible through two identical carbonyl-fringed portals.[1] Its hydrophobic cavity and polar carbonyl groups at the portals allow CB[6] to form stable host−guest complexes with a wide range of molecules and ions such as protonated aminoalkanes.[2−10] In particular, it forms very stable complexes with protonated polyamines,[11−13] which is almost comparable to that of biotin−avidin system. The strong and specific interaction makes it one of the affinity pairs widely used in many applications such as immunological and theranostic systems.[14] In particular, it is a useful noncovalent conjugation tool and extensively used for immobilizing a wide variety of tags or functional moieties, such as targeting ligands and imaging probes by highly stable host−guest chemistry.[15−21]

These results prompted us to develop CB[6]-anchored polymers as multifunctional active materials. An apparent advantage of CB[6]-anchored polymers is the appearance of CB[6] cavity on the polymer backbone, which allows the tailoring of polymer properties for the special applications or introduction of functional moieties.[14,22,23]

In addition, much more novel properties of CB[6]-anchored polymers were presented in the fields like macromolecular machines, smart materials and molecular assemblies. These novel properties make CB[6]-anchored polymers useful in chromatographic fillers, membranes and drug carrier systems.[15,17−19,22,24−32] However, the covalent linkage of between CB[6] and polymer chains can not be performed easily, and thus their applications are limited. In order to bond CB[6] into polymer backbone, reactive functional groups must be appended on the CB[6] surface, which mostly requires laborious, often low yield syntheses.[20,28] Our efforts have been focused on developing a facile method for synthesis of CB[6]-anchored polymers.

Herein, we explored one-pot, direct method for the preparation of CB[6]-anchored polymers without the functionalization of CB[6], which seems to be applicable to the monomers of radical polymerization in aqueous solution. Acrylamide was used as a typical monomer to investigate the details. A series of CB[6]-anchored polyacrylamide (CB[6]-PAM) were synthesized in aqueous solution using potassium persulfate (KPS) as initiator and oxidant. The composition, microstructure and morphologies of CB[6]-PAM could be controlled by changing the content of potassium persulfate, CB[6] and acrylamide. The content of CB[6] varies from approximately 0.012 to 0.02 g/mL. CB[6]-anchored polyacrylamide was successfully assembled into nanosized vesicles. The nanosized vesicles, once noncovalently modified with targeting ligands, could demonstrate their potential as a targeted drug delivery vehicle. ^{1}H NMR, ^{13}C NMR, HMQC, FTIR, and TGA were used for characterization of CB[6]-PAM. The morphology of CB[6]-PAM based aggregates was observed and confirmed by TEM, AFM, and SEM measurements. In addition, this synthetic approach can be extend to CB[6]-anchored polymer with two different chains. As an

Received: January 4, 2013
Revised: January 26, 2013
Published: February 14, 2013

dx.doi.org/10.1021/ma400017y | *Macromolecules* 2013, 46, 1274−1282

example, CB[6]-anchored poly(4-vinylbenzylamine hydrochloride salt) and polyacrylamide (CB[6]-PAM-PVBAHS) was prepared.

EXPERIMENTAL SECTION

Materials. CB[6] and 4-vinylbenzylamine hydrochloride salt were prepared according to the literature.[33,34] Potassium persulfate (AP) and butyl amine (AP) were received from Shanghai Reagent Company . Acrylamide (AR) from Beijing Chemical Reagent Co. was further purified by three-time recrystallization.

Synthesis of CB[6]-Anchored Polyacrylamide. In a typical experiment, 0.5 g CB[6] and 0.324 g of potassium persulfate were dispersed in 25 mL of distilled water, and stirred for 5 min at room temperature. The solution was stirred with a small magnetic stir bar under an inert N_2 atmosphere and heated to 80 °C with an oil bath. After thermal equilibrium had been reached, the solution was bubbled with N_2 for about 0.5 h, then 0.4 mol/L aqueous solution of acrylamide was added by drop funnel. After 8 h, the solution was cooled to room temperature. The resulting precipitate was removed by filtration. The filtrate was purified by dialysis (MWCO 3000) against water for 24 h to give a solution of polymer, which was concentrated to 10 mL under the reduced pressure. The concentrated solution was precipitated with acetone, then dissolution−precipitation three times. The final precipitation was collected, dipped in acetone for 4 h and dried under reduced pressure at 40 °C for 48 h. The other CB[6]-anchored polyacrylamide samples were synthesized under the similar conditions except for the feed mass of CB[6], acrylamide, and potassium persulfate, which are listed in Table 1.

Table 1. Feeding Composition of CB[6]-PAM Samples

samples	CB[6] (g/mL)	AM (moL/L)	KPS (g/mL)	feed mole ratio of KPS/active sites of CB[6]
CB[6]-PAM-1	0.012	0.4	0.013	0.33
CB[6]-PAM-2	0.016	0.4	0.013	0.25
CB[6]-PAM-3	0.020	0.4	0.013	0.20
CB[6]-PAM-4	0.020	0.2	0.013	0.20
CB[6]-PAM-5	0.020	0.6	0.013	0.20
CB[6]-PAM-6	0.020	0.4	0.019	0.30

Noncovalent Modification of CB[6]-Anchored Polyacrylamide with Protonated Aminoalkanes. CB[6]-PAM was dissolved in 20 mL of H_2O, and stirred for 10 min at room temperature. Then, excess amount of butyl amine hydrochloride was slowly dripped to the solution and stirred for 2 h at room temperature. The reaction solution was precipitated with methanol. The white precipitation was washed three times with methanol and dried under reduced pressure at 40 °C for 48 h.

Characterization. All ^1H NMR, ^{13}C NMR, and HMQC experiments were performed on a Bruker AVANCEIII-500 NMR spectrometer. D_2O was used for field-frequency lock, and the observed chemical shifts are reported in parts per million (ppm) relative to an internal standard (TMS, 0 ppm).

Fourier-transform infrared (FTIR) was carried out on a NEXUS-670 (Nicolet, American) with sample prepared as KBr pellets. The spectra were acquired in the frequency range 4000−400 cm^{-1} at a resolution of 4 cm^{-1} with a total of 16 scans.

Thermal characteristics of samples were determined with a thermogravimetric analyzer (TGA). TGA was performed with a STA409PC TGA system (Netzsch, Germany). The analysis was performed with approximately of 10 mg of dried samples in a dynamic nitrogen atmosphere (flow rate 50 mL/min) at a heating rate of 10 °C/min.

High-resolution transmission electron microscopy (TEM) images were recorded on a JEM-2010F electron microscope operated at 200 KV. Samples were immobilized on copper grids covered with carbon. The samples were stained with 20% of phosphotungstic acid, and the specimens were dried at room temperature before examination.

Atomic force microscopy (AFM) images were recorded on a CSPM5500−0034 AFM (Beijing Nano-Insturments, Ltd.). Dilute sample solution was spin-coated onto a silicon wafers and allowed to dry in a vacuum desiccator for several hours. Images were obtained using tapping-mode, with Olympus AC 240 tips.

Scanning electron microscopy (SEM) images were carried out on a Hitachi S4800 field-emission SEM system. Dilute sample solution was immobilized onto a silicon wafers and allowed to dry in a vacuum desiccator for several hours. The specimens were treated by spray gold.

GPC measurements were carried out in 0.1 M phosphate buffer solution eluent (pH 6.8, 1 mL/min) at 30 °C using a Waters 515 liquid chromatography equipped with two gel permeation chromatography columns in series (Waters Ultrahydrogel 500, 7.8 mm ×300 mm and Waters Ultrahydrogel 250, 7.8 mm ×300 mm) with a refractive index detector.

RESULTS AND DISCUSSION

Synthesis Strategy. It is well-known that reaction of CB[6] with excess potassium persulfate in water produces hydroxyl derivatives of CB[6].[20] Although the hydroxylation mechanism of CB[6] has not been fully understood, it is possible that the addition of potassium persulfate to the system produces hydroxyl radicals and simultaneously generates new radicals on the surface of CB[6].[28] It is our suggestion that the direct functionalization method of CB[6] was compatible with a radical polymerization technique in aqueous solution. The produced radicals on the surface of CB[6] could take part in the initiation, propagation, termination or transfer reaction of

Scheme 1. Synthesis Strategy of CB[6]-Anchored Polyacrylamide by Free Radical Reaction in Aqueous Solution

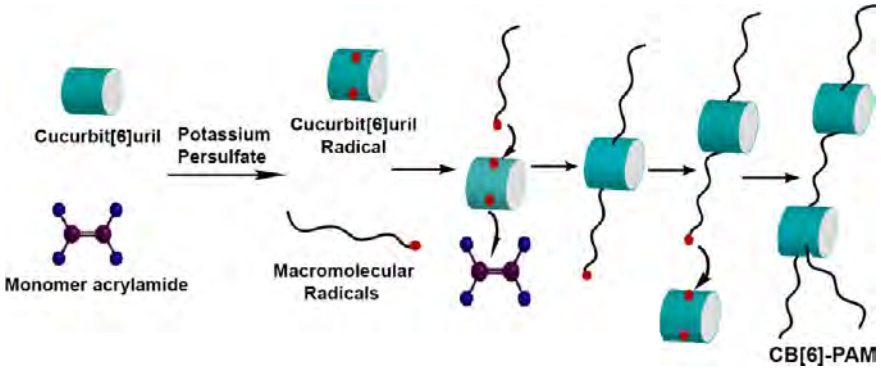

dx.doi.org/10.1021/ma400017y | Macromolecules 2013, 46, 1274−1282

vinyl polymerization. Therefore, functionalization of CB[6] and polymerization of monomer could be carried out simultaneously via one-pot, direct radical polymerization method. To obtain CB[6]-anchored polymer via direct radical polymerization method, the most two important factors should be taken into account: the macromolecular backbone and construction method. In this paper, we chose the polyacrylamide as macromolecular backbone. As to the synthesis methods, we selected the common free radical reaction in aqueous solution to construct the CB[6]-anchored polyacrylamide due to its simplicity and generality. The synthesis strategy is illustrated in Scheme 1 and the procedure is surprisingly simple.

After initiating of vinyl monomers, macromolecular radicals are formed immediately by chain propagation. If the macromolecular radicals are coupled to the radical on the surface of CB[6], the CB[6]-PAM polymer chains could be prepared. Meanwhile, the radicals on the surface of CB[6] are also liable to further radical initiation, propagation, and termination, producing CB[6]-anchored polyacrylamide. In addition, it should be pointed out that 12 active sites of CB[6] can be obtained by the reaction of excess potassium persulfate.[35] When newly generated macromolecular radicals are further bonded to the active sites of CB[6]-PAM, star, or branched polymer chains would formed. Thus, by changing the molar ratio of CB[6] to potassium persulfate, the polymer microstructure was able to be controlled.

Synthesis Exploring. Six CB[6]-PAM samples were synthesized via free radical polymerization in aqueous solution using potassium persulfate as initiator and oxidant. They were polymerized under identical conditions except for the feed mass of CB[6], acrylamide (AM), and potassium persulfate (KPS), which are shown in Table 1.

The obtained CB[6]-PAM samples were characterized by ^{1}H NMR, ^{13}C NMR, HMQC, FTIR, and TGA techniques. The successful synthesis of CB[6]-anchored polyacrylamide was confirmed by NMR analysis. The ^{13}C NMR spectrum[20,36−38] of the CB[6]-PAM-3 polymer confirmed that the typical amide carbonyl carbon (−CO-NH$_2$) signal appeared at δ 179.5 ppm. The resonances of two different carbonyl carbons at 156.2 and 154.7 ppm were assigned to the polyacrylamide grafted and ungrafted glycoluril units of CB[6][20] respectively, suggesting that two kinds of glycoluril units of CB[6] were obtained. No bis(polyacrylamide)-grafted glycoluril units were observed. In addition, The presence of signal at δ 39.8−40.7 ppm was the methylene carbons of polyacrylamide segment grafted to oxygen of CB[6]-O- units, which confirmed the formation of new CB[6]-O-polyacrylamide linkages (Figure S1, Supporting Information). The C,H-COSY NMR spectrum showed the protons at δ 5.17−5.28 ppm correlated with carbon signals at δ 39.81−40.75 ppm, which were assigned to the methylene protons of polyacrylamide segment grafted to oxygen of CB[6]-O− units (Figure S2, Supporting Information).[20,36−39] However, the signals at δ 5.17−5.28 ppm were overlapped with the methine protons of grafted glycoluril units in part in ^{1}H NMR spectrum (Figure S3, Supporting Information). From above results, it is reasonable to conclude that CB[6]-anchored polyacrylamide was synthesized successfully. Furthermore, the FTIR spectra of CB[6]-PAM samples revealed two characteristic peaks at 1667 and 1750 cm^{-1}, corresponding to the carbonyl moiety of the polyacrylamide chains and CB[6] (Figure S4, Supporting Information). The TGA curves (Figure S5, Supporting Information) of CB[6]-PAM sample showed three weight loss stages. The first stage at about 250 °C resulted from the decomposition of the amide groups of grafted PAM chains. This decomposition temperature is somewhat lower than that of neat PAM (287 °C). The second stage of CB[6]-PAM samples at about 375 °C was attributed to the main decomposition of grafted PAM. The third transition of CB[6]-PAM samples is observed at about 470 °C, which was assigned to the decomposition of CB[6] groups of CB[6]-PAM. In contrast, the decomposition temperature of neat CB[6] is higher than that of CB[6] groups of CB[6]-PAM.[6,40] These results further indicated that the PAM chains have been successfully grafted on CB[6] through the in situ radical polymerization approach.

Effect of the Different Polymerization Conditions on the Formation of CB[6]-PAM. Table 2 listed all the results of the six CB[6]-PAM samples. The $\bar{M}_w$ for the CB[6]-PAM samples showed only slight variation with the variation of feed condition as listed in Table 2. The typical GPC plot of CB[6]-PAM-1 in phosphate buffer solution indicated a significant branching phenomenon under these reaction conditions,[41] which was because the 12 oxidizable sites at the periphery of CB[6] could bond with polymer chains to grow into branched polymer chains (Figure S6, Supporting Information).

Table 2. Composition and $\bar{M}_w$ of CB[6]-PAM Samples

samples	grafting degree of CB[6]	PAM/CB[6]	$\bar{M}_w$ (10^4 g/moL)
CB[6]-PAM-1	0.47	55:1	25
CB[6]-PAM-2	0.40	41:1	18
CB[6]-PAM-3	0.33	29:1	23
CB[6]-PAM-4	0.36	15:1	15
CB[6]-PAM-5	0.35	67:1	34
CB[6]-PAM-6	0.48	34:1	20

For the six samples of CB[6]-PAM obtained at different polymerization conditions, the average molar ratio of repeating unit of PAM to CB[6] unit (PAM/CB[6]) and the average molar ratio of grafted glycoluril units to all the glycoluril units of CB[6] (average grafting degree of CB[6]) were characterized by ^{1}H NMR (Figure S3, Supporting Information). All the results for the six CB[6]-PAM samples are listed in Table 2.

To understand the effect of the CB[6] concentration on the average grafting degree of CB[6], we used the initial CB[6] concentration of 0.012, 0.016, and 0.020 g/mL in the syntheses of polymers CB[6]-PAM-1, CB[6]-PAM-2 and CB[6]-PAM-3 as listed in Table 1. The differences of average the grafting degree of CB[6] among CB[6]-PAM-1, CB[6]-PAM-2, and CB[6]-PAM-3 could be observed as shown in Figure 1 and the results are listed in Table 2.

The results revealed that the larger concentration of CB[6] produces lower grafting degree of CB[6] (CB[6]-PAM-3, average grafting degree 0.33), whereas the smaller concentration of CB[6] yields higher grafting degree of CB[6] (CB[6]-PAM-1, average grafting degree 0.47) under the same condition.

On the basis of the procedure proposed in Scheme 1, at the early stage of reaction, CB[6] with 12 oxidizable site at the periphery react with potassium persulfate to form radicals on the surface of CB[6], which further react with monomers or macromolecular radicals to grow into CB[6]-anchored PAM. As the amount of CB[6] decreases at the constant amount of potassium persulfate, the average number of the reaction site of

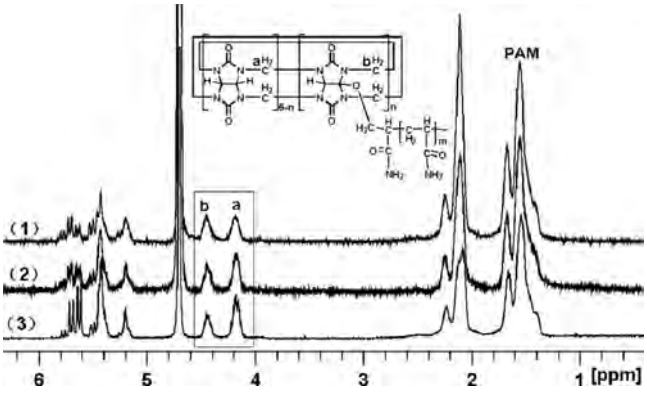

Figure 1. ^{1}H NMR spectra of (1) CB[6]-PAM-1, (2) CB[6]-PAM-2, and (3) CB[6]-PAM-3.

per CB[6] units increases. As a result, the increased site of per CB[6] enhanced the grafting degree of CB[6].

However, the reaction carried out with a concentration of CB[6] below 0.008 g/mL generated only gelation, indicating that there is a critical concentration for the CB[6]. When the concentration of CB[6] is lower than the critical concentration, CB[6] units would produce a highly cross-linked polymer, leading to the occurrence of gelation.

The CB[6] concentration also significantly affected PAM/CB[6] value as shown in Table 2. As can be seen, PAM/CB[6] value decreases with increasing the CB[6] concentration. The FTIR spectra also revealed that the relative intensity of the peak at 1667 cm^{-1} to 1750 cm^{-1} decreases gradually with the increasing amount of CB[6] (shown with arrows in Figure S4, Supporting Information), suggesting PAM/CB[6] values decreased in the order of CB[6]-PAM-1, CB[6]-PAM-2, and CB[6]-PAM-3. From the DTGA curves of CB[6]-PAM-1, CB[6]-PAM-2, and CB[6]-PAM-3 (Figure S7, Supporting Information), we clearly find that the PAM/CB[6] value play an important role for decomposition temperature of amide groups. The DTGA curves indicated notably that the decomposition temperature of the amide groups of grafted PAM decreases with the decrease of PAM/CB[6] values. This deviation was due to the fact that the bulky steric hindrance of CB[6] hinders the formation of hydrogen bonds between the amide groups, leading to the decrease of decomposition temperature of amide groups with the increase of CB[6] amount.[41]

Another important factor to influence the formation of CB[6]-PAM is the acrylamide concentration. When we increased the concentration of reactant acrylamide in the reaction mixture at the constant molar ratio of CB[6] to KPS (1:0.2), the average PAM/CB[6] value increased, as indicated in Table 2.

For example, the radical reaction carried out at different acrylamide concentration of 0.2, 0.4, and 0.6 M as shown in Table 1, produced the polymer with the average PAM/CB[6] of 15:1, 29:1 and 67:1, respectively (Table 2, CB[6]-PAM-4, CB[6]-PAM-3, and CB[6]-PAM-5). However, the average grafting degrees of CB[6] have no evident difference.

The results indicated that the composition of the CB[6]-PAM polymer could be systematically controlled by the concentration of acrylamide. In general, the higher the

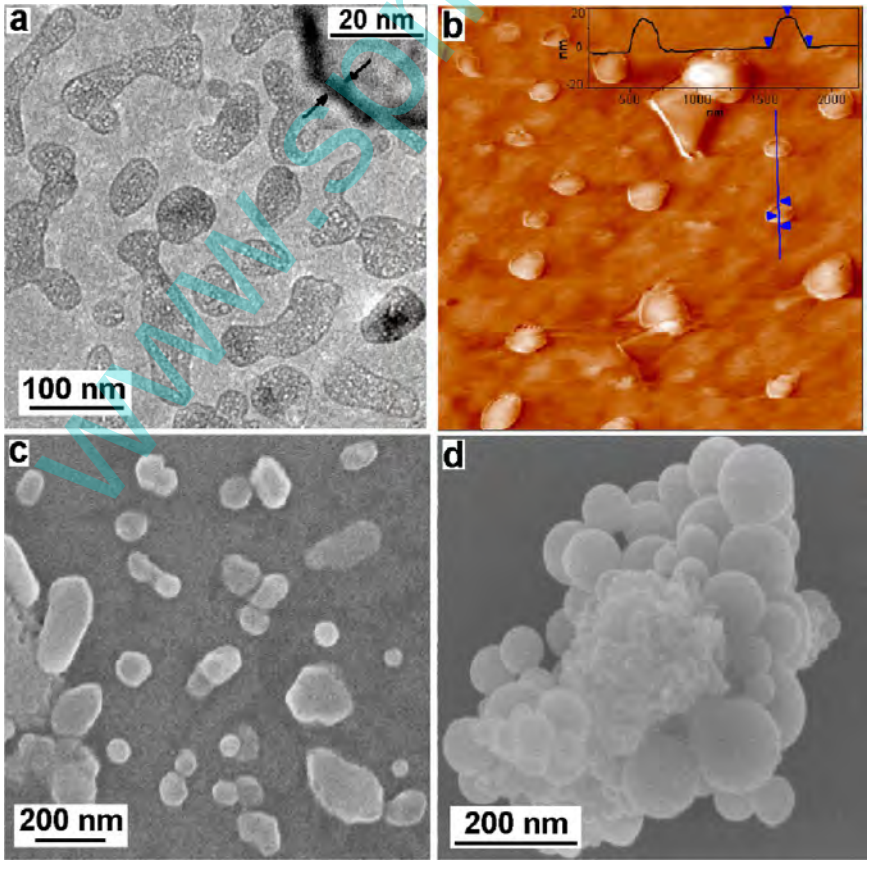

Figure 2. Images of CB[6]-PAM-1 aggregates (a, TEM; b, AFM; c and d, SEM).

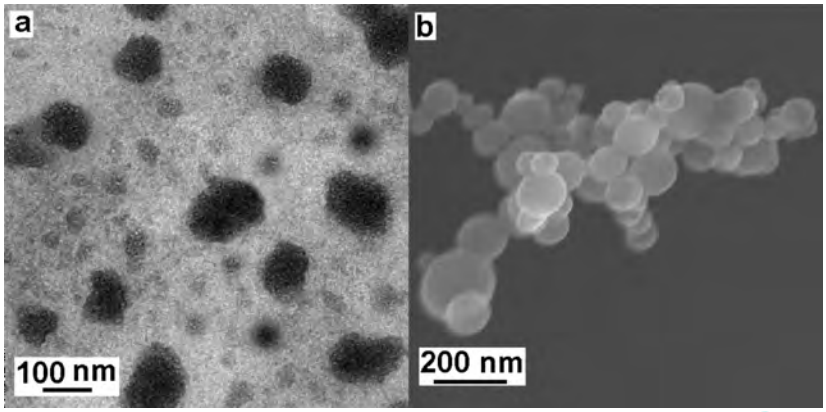

Figure 3. Images of CB[6]-PAM-6 aggregates (a, TEM; b, SEM).

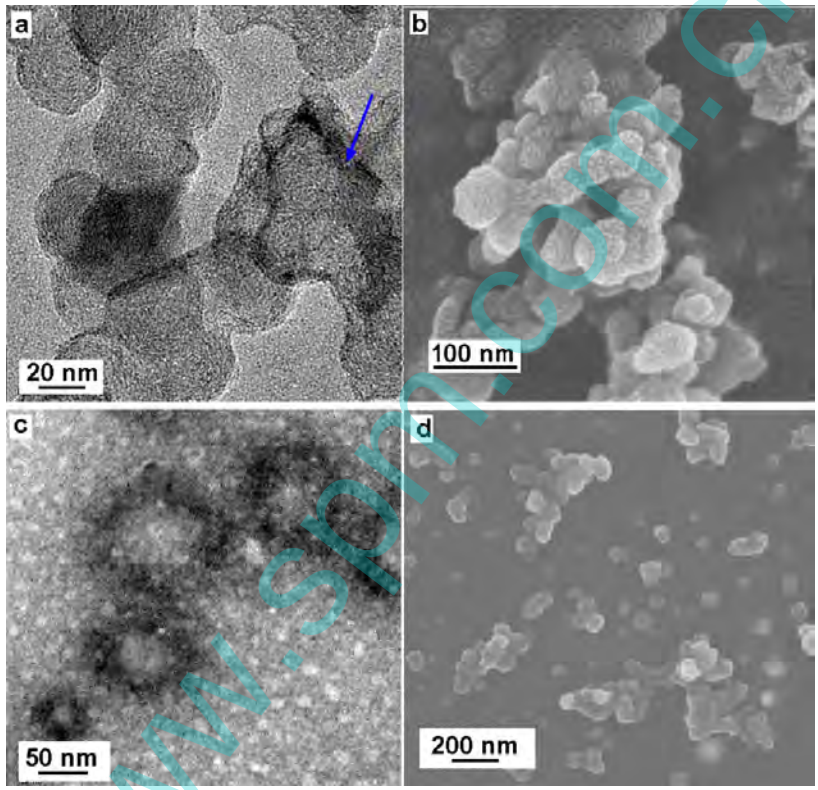

Figure 4. Aggregate morphology of CB[6]-PAM-4 (a, TEM; b, SEM) and CB[6]-PAM-5 (c, TEM; d, SEM).

acrylamide concentration was, the more the repeating unit of PAM grafted, which is consistent with the theory of radical polymerization.

Size and Morphology of the CB[6]-Anchored Polyacrylamide. The size and morphlolgy of the polymer aggregates are important factors for their applications.[41] Here, the morphology of CB[6]-PAM-based aggregates were studied by TEM, AFM, and SEM measurements.

Figure 2, Figure 3, and Figure 4 show the representative micrographs of aggregates formed from the different CB[6]-PAM polymer samples under the same condition. Our examination of many images concludes that the size and micrograph of aggregates could be systematically controlled by the grafting degree of CB[6] and the ratio of PAM/CB[6].

According to the results of the ^{1}H NMR listed in Table 2, the grafting degree of CB[6] of CB[6]-PAM-1 and CB[6]-PAM-6 are approximately close and higher than other samples.

Figure 2 presents a set of images which show the morphology of aggregates prepared from CB[6]-PAM-1 sample. From TEM image of CB[6]-PAM-1 (Figure 2 a), we can see that the aggregates were much more polydisperse and contained many kinds of vesicles. Most of the aggregates were large elongated compound vesicles with the thickness of the membrane about 6 nm. Small spherical vesicles aggregates with diameter of 100−200 nm were also observed. The size and morphlolgy of the polymer aggregates were further measured by AFM. Tapping-mode AFM of CB[6]-PAM-1 (Figure 2 b) showed flattened and elongated spheres with the size of 100−300 nm and a height of 15−20 nm. SEM of CB[6]-PAM-1 in Figure 2, parts c and d, confirmed the coexistence of the large elongated compound vesicles and small spherical vesicles aggregates, which nicely match the results observed by TEM and AFM.

Scheme 2. Formation Model of the CB[6]-PAM-Based Vesicle

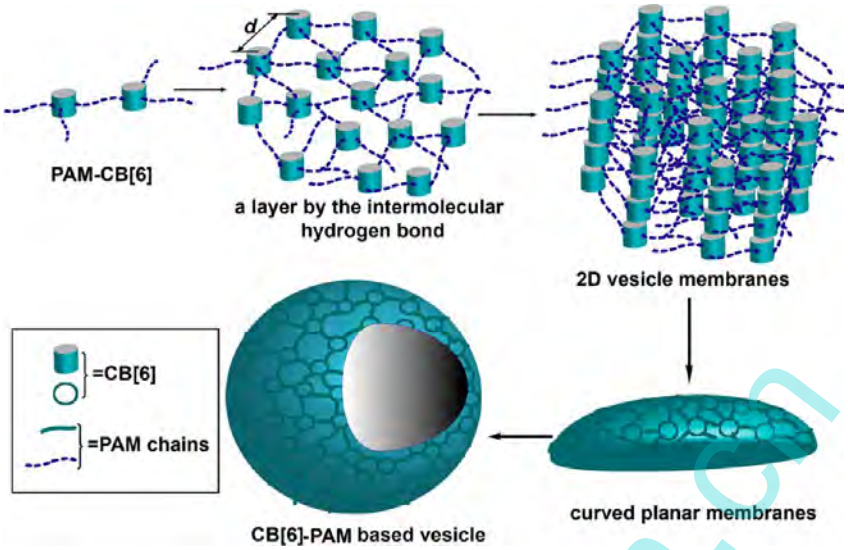

The similar large compound vesicles together with many small vesicles for CB[6]-PAM-6 aggregates were observed by TEM and SEM (Figure 3, parts a and b), but most of the aggregates became more spherical and their average size was smaller than that of CB[6]-PAM-1 sample.

The aggregate morphology of CB[6]-PAM-4 and CB[6]-PAM-5 with different PAM/CB[6] ratios were observed by TEM and SEM as shown in Figure 4. Parts a and b of Figure 4 show planar lamella structure of CB[6]-PAM-4 with diameter of 100 nm. As seen from TEM images, some of the lamellae have curved edges, such as those indicated in Figure 4a by an arrow. For CB[6]-PAM-5 sample, with higher ratio of PAM/CB[6], vesicular aggregates with diameter of 100 nm were observed by TEM and SEM (Figure 4, parts c and d).

Proposed Model of the Nanocapsule Formation. On the basis of the above observations and the general formation mechanism of vesicles, we proposed a model for the formation of the nanocapsule. The proposed model is similar to the formation model of lipid vesicles, in which the planar bilayers are assumed to be involved. Under certain conditions, the planar bilayers are more favorable for closed bilayer (vesicles) rather than infinite planar bilayers. It is because the energetically unfavorable edges in a closed bilayer are eliminated at a finite aggregation number, which is also entropically favored.[42]

The proposed model for the formation of CB[6]-PAM based planar layers is shown in Scheme 2, which includes the formation of a layer by the intermolecular hydrogen bonds between the amide and the carbonyl group of CB[6] portals (N−H...O═C),[6,18] and stacking such layers to form the 2D vesicle membranes. Such 2D planar membranes start to bend to reduce their total energy. Thus, so long as the CB[6]-PAM in a curved planar membranes can maintain their parameters such as PAM/CB[6] and grafting degree of CB[6] at their optimal value, vesicles should be the preferred structures.[42]

According to the theoretical model reported by Israelachvili et al.,[42] the radius of the formed smallest vesicle is defined as the critical radius (R_c), below which a bilayer cannot curve without introducing unfavorable packing strains. Namely, for $R < R_c$, such vesicles are energetically unfavored.[42] Kimoon Kim et al. have developed the theoretical model of Israelachvili to understand the CB[6] based polymer nanocapsules formation, including the energy and size distribution of nanocapsules.[17]

On the basis of the theory of Kim, the critical radius R_c of CB[6]-based polymer nanocapsules is $d(\pi\kappa/6\varepsilon)^{1/2}$. Here d is the distance between two CB[6] units in the aggregates, ε is the bond energy per linkage and κ is the bending rigidity.

In general, d and κ can be systematically controlled by the PAM/CB[6] and grafting degree of CB[6]. As can be seen, as the number of molar ratio of PAM/CB[6] increases, the average distance between two CB[6] units d increases. Meanwhile, the length of PAM chains between two CB[6] units and grafting degree of CB[6] can change the bending rigidity κ.

Considering the size of the aggregates formed in the self-assembly process, Kim proposed the average radius is

$$\langle R\rangle = \int \mathrm{d}R\ RP(R) = \frac{\pi}{8} dC^{1/4} \mathrm{e}^{2\pi\kappa/KT}$$

The equation suggests that changes in the distance between neighboring CB[6] units d and bending rigidity κ affect the average size of aggregates.

Thus, under certain conditions of d and κ, no stable vesicles should form; instead, extended bilayers should occur, which is in good agreement with the experimental results as described.

Noncovalent Modification of CB[6]-PAM. One of the unique properties of the CB[6]-anchored polymer described here is the CB[6] cavity appeared on the polymer backbone. By taking advantage of the exceptional binding affinity of polyamine on the CB[6], the CB[6]-PAM can be readily modified with various functional "tags" by using tag-polyamine conjugates in a noncovalent manner.

In this paper, we investigated the modification of CB[6]-PAM using butyl amine hydrochloride, which forms a stable 1:1 complex with CB[6]. The successful modification of CB[6]-PAM with butyl amine hydrochloride was confirmed by ^{1}H NMR as shown in Figure 5(2). The ^{1}H NMR spectrum of the complex of CB[6] and butyl amine hydrochloride is shown in Figure 5(1) for comparison.

It reveals that upon formation of the complex between CB[6]-PAM and butyl amine hydrochloride, the methyl and methylene signals of butyl amine hydrochloride are upfield-shifts due to the shielding effect of CB[6], which are the

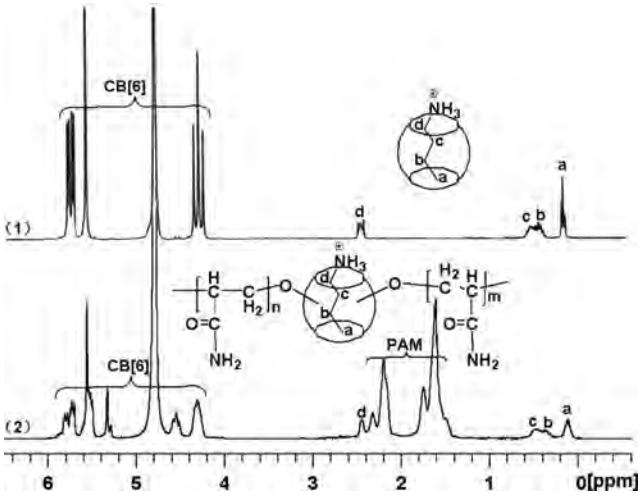

Figure 5. ^{1}H NMR spectra of (1) the complex of CB[6] and butyl amine hydrochloride and (2) butyl amine hydrochloride modified CB[6]-PAM.

consistent with the complex of CB[6] and butyl amine hydrochloride. In addition, no apparent change on the morphology of the CB[6]-PAM aggregates was observed after they were treated with butyl amine hydrochloride. These results confirmed that the functional "tags", if they are attached to aminoalkane, can be introduced to the CB[6]-anchored polymer in a noncovalent manner, which makes the CB[6]-anchored polymer potentially useful in many applications, including targeted delivery.

Extension of the Synthesis Strategy. The above CB[6]-PAM cases have sufficiently shown the feasibility and simplicity of our synthesis strategy. To demonstrate the generality of our strategy, we conducted experiments to extend it to other monomers. The synthesis strategy of CB[6]-anchored polymers with two different chains is illustrated in Scheme 3.

For example, reaction of CB[6]-PAM with 4-vinylbenzylamine hydrochloride salt (VBAHS) in the presence of KPS at 80 °C produced CB[6]-anchored poly(4-vinylbenzylamine hydrochloride salt) and polyacrylamide (CB[6]−PAM-PVBAHS), which was confirmed by ^{1}H NMR spectrum as shown in Figure 6.

The CB[6]−PAM-PVBAHS shows the pH-responsive behavior. The vesicular aggregates of CB[6]-PAM-PVBAHS with diameter of 300−400 nm in pH = 3 solution were observed by TEM and AFM as shown in Figure 7. The kind of CB[6]-PAM-PVBAHS with pH-stimulant responsive properties has their great potentials in both academic theory and

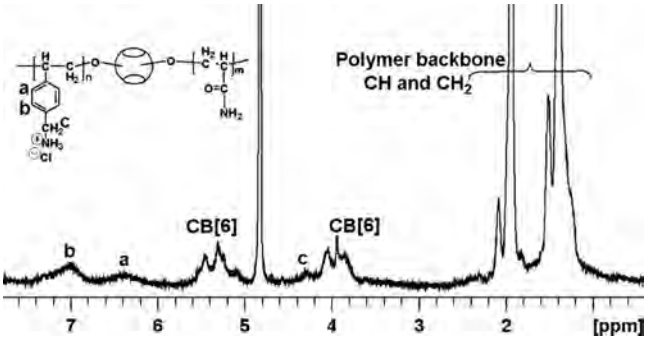

Figure 6. ^{1}H NMR spectrum of CB[6]-PAM-PVBAHS.

application fields, the details of which will be published separately.

CONCLUSION

In summary, we have developed a facile, reliable, and general strategy for synthesis of CB[6]-anchored polymers, which does not require the functionalization of CB[6]. The synthesis strategy seems to be applicable to the monomer of radical polymerization in aqueous solution. In this paper, the acrylamide as the typical monomer was used to synthesize a series of CB[6]-anchored polyacrylamide (CB[6]-PAM) in aqueous solution. The chemical structures of the obtained CB[6]-PAM samples were confirmed by ^{1}H NMR, ^{13}C NMR and HMQC. The results of ^{1}H NMR revealed that the composition and chain microstructure of CB[6]-PAM polymers could be controlled by changing the content of potassium persulfate, CB[6] and acrylamide. The larger concentration of CB[6] produces a lower grafting degree of CB[6] (CB[6]-PAM-3, average grafting degree 0.33), whereas the smaller concentration yields a higher grafting degree of CB[6] (CB[6]-PAM-1, average grafting degree 0.47) under the same condition. In general, the ratio of PAM/CB[6] increased with the increase of acrylamide concentration. On the basis of a number of observations including TEM, AFM and SEM measurements, we can see that the size and morphology of aggregates could be systematically controlled by the grafting degree of CB[6] and the ratio of PAM/CB[6]. For different grafting degree of CB[6] and PAM/CB[6] ratios, the vesicles and planar lamellae with different size and morphology could be observed.

One of the interesting properties of the CB[6]-anchored polymer was that the CB[6] cavity appeared on the polymer backbone allows facile tailoring of its properties in a noncovalent manner by virtue of the unique recognition

Scheme 3. Proposed Synthesis Strategy of CB[6]-Anchored Polymers with Two Different Chains

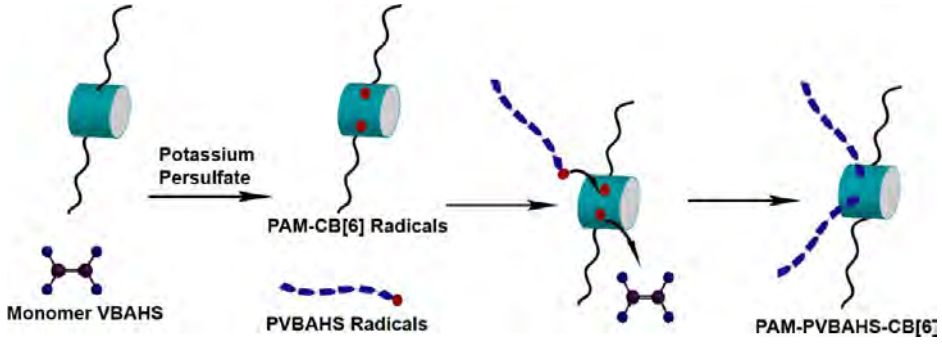

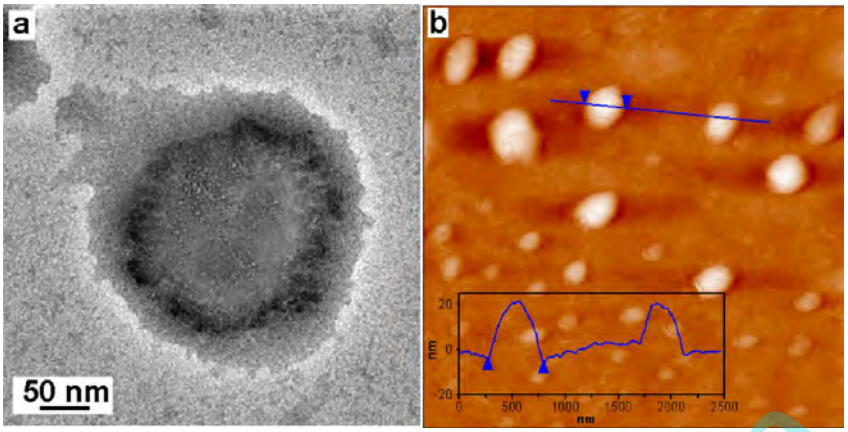

Figure 7. Image of CB[6]-PAM-PVBAHS vesicular aggregates.

properties of CB[6]. In this paper, the successful modification of CB[6]-PAM with butyl amine hydrochloride was confirmed by ^{1}H NMR. These results confirmed that the functional "tags", if they are attached to polyamines, can be introduced to the CB[6]-anchored polymer in a noncovalent manner, which makes the CB[6]-anchored polymer potentially useful in many applications, including targeted delivery.

Furthermore, this synthetic approach appeared to be applicable to other vinyl monomers and could be extend to CB[6]-anchored polymers with two different polymer chains. As a example, reaction of CB[6]-PAM with 4-vinylbenzylamine hydrochloride salt produced the CB[6]-anchored poly(4-vinylbenzylamine hydrochloride salt) and polyacrylamide (CB[6]-PAM-PVBAHS). This novel synthesis approach for CB[6]-anchored polymers has their great potentials in both academic theory and application fields.

■ ASSOCIATED CONTENT

Supporting Information

Additional ^{13}C NMR spectrum, C, H−COSY NMR spectrum, ^{1}H NMR spectrum, FTIR spectra, and GPC, TGA, and DTGA curves. This material is available free of charge via the Internet at http://pubs.acs.org.

■ AUTHOR INFORMATION

Corresponding Author

*Telephone: +86 471 4992979. Fax: +86 471 4992979. E-mail: haiquansu@yahoo.com.

Notes

The authors declare no competing financial interest.

■ ACKNOWLEDGMENTS

This work was financially supported by the National Natural Science Foundation of China (No. 51103067) and Inner Mongolia Natural Science Foundation (No. 2010BS0803).

■ REFERENCES

(1) Lagona, J.; Mukhopadhyay, P.; Chakrabarti, S.; Isaacs, L. *Angew. Chem., Int. Ed.* **2005**, *44*, 4844−4870.
(2) Thuéry, P. *Cryst. Growth Des.* **2011**, *11*, 3282−3294.
(3) Thuéry, P. *Inorg. Chem.* **2011**, *50*, 10558−10560.
(4) Xiao, X.; Wang, Q.; Yu, Y.-H.; Xiao, Z.-Y.; Tao, Z.; Xue, S.-F.; Zhu, Q.-J.; Liu, J.-X.; Liu, X.-H. *Eur. J. Org. Chem.* **2011**, *2011*, 2366−2371.
(5) El-Barghouthi, M.; Assaf, K.; Rawashdeh, A. *J. Chem. Theory Comput.* **2010**, *6*, 984−992.
(6) Huang, X.; Tan, Y.; Wang, Y.; Yang, H.; Cao, J.; Che, Y. *J. Polym. Sci., Part A: Polym. Chem.* **2008**, *46*, 5999−6008.
(7) Isobe, H.; Tomita, N.; Lee, J.; Kim, H.; Kim, K.; Nakamura, E. *Angew. Chem., Int. Ed.* **2000**, *39*, 4257−4260.
(8) Zhang, F.; Yajima, T.; Li, Y.-Z.; Xu, G.-Z.; Chen, H.-L.; Liu, Q.-T.; Yamauchi, O. *Angew. Chem., Int. Ed.* **2005**, *117*, 3468−3473.
(9) Buschmann, H.-j.; Mutihac, L.; Schollmeyer, E. *J. Inclusion Phenom. Macrocycl. Chem.* **2005**, *53*, 85−88.
(10) Pessêgo, M.; Moreira, J. a.; Garcia-Rio, L. *Chemistry (Weinheim, Germany)* **2012**, *18*, 7931−7940.
(11) Rekharsky, M.; Ko, Y. H.; Selvapalam, N.; Kim, K.; Inoue, Y. *Supramol. Chem.* **2007**, *19*, 39−46.
(12) Zhang, S.; Echegoyen, L. *Org. Lett.* **2004**, *6*, 791−794.
(13) Kim, J.; Kim, Y.; Baek, K.; Ko, Y.; Kim, D.; Kim, K. *Tetrahedron* **2008**, *64*, 8389−8393.
(14) Jung, H.; Park, K. M.; Yang, J.-A.; Oh, E. J.; Lee, D.-W.; Park, K.; Ryu, S. H.; Hahn, S. K.; Kim, K. *Biomaterials* **2011**, *32*, 7687−7694.
(15) Kim, E.; Kim, D.; Jung, H.; Lee, J.; Paul, S.; Selvapalam, N.; Yang, Y.; Lim, N.; Park, C. G.; Kim, K. *Angew. Chem., Int. Ed.* **2010**, *49*, 4405−4408.
(16) Kim, J.; Ahn, Y.; Park, K. M.; Lee, D.-W.; Kim, K. *Chem.—Eur. J.* **2010**, *16*, 12168−12173.
(17) Kim, D.; Kim, E.; Lee, J.; Hong, S.; Sung, W.; Lim, N.; Park, C.; Kim, K. *J. Am. Chem. Soc.* **2010**, *132*, 9908−9919.
(18) Park, K. M.; Lee, D.-W.; Sarkar, B.; Jung, H.; Kim, J.; Ko, Y. H.; Lee, K. E.; Jeon, H.; Kim, K. *Small* **2010**, *6*, 1430−1441.
(19) Park, K. M.; Suh, K.; Jung, H.; Lee, D.-W.; Ahn, Y.; Kim, J.; Baek, K.; Kim, K. *Chem. Commun.* **2009**, 71−73.
(20) Jon, S.; Selvapalam, N.; Oh, D.; Kang, J.; Kim, S.; Jeon, Y.; Lee, J.; Kim, K. *J. Am. Chem. Soc.* **2003**, *125*, 10186−10187.
(21) Taylor, R. W.; Lee, T.-C.; Scherman, O. a.; Esteban, R.; Aizpurua, J.; Huang, F. M.; Baumberg, J. J.; Mahajan, S. *ACS Nano* **2011**, *5*, 3878−3887.
(22) Nagarajan, E. R.; Oh, D. H.; Selvapalam, N.; Ko, Y. H.; Park, K. M.; Kim, K. *Tetrahedron Lett.* **2006**, *47*, 2073−2075.
(23) Shen, C.; Ma, D.; Meany, B.; Isaacs, L.; Wang, Y. *J. Am. Chem. Soc.* **2012**, *134*, 7254−7257.
(24) Cheong, W.; Go, J.; Baik, Y.; Kim, S.; Nagarajan, E.; Selvapalam, N.; Ko, Y.; Kim, K. *Bull. Korean Chem. Soc.* **2008**, *29*, 1941−1945.
(25) Kim, E.; Lee, J.; Kim, D.; Lee, K. E.; Han, S. S.; Lim, N.; Kang, J.; Park, C. G.; Kim, K. *Chem. Commun.* **2009**, 1472−1474.
(26) Kim, D.; Kim, E.; Kim, J.; Park, K. M.; Baek, K.; Jung, M.; Ko, Y. H.; Sung, W.; Kim, H. S.; Suh, J. H.; Park, C. G.; Na, O. S.; Lee, D.-k.; Lee, K. E.; Han, S. S.; Kim, K. *Angew. Chem., Int. Ed.* **2007**, *46*, 3471−3474.
(27) Kim, J.; Ahn, Y.; Park, K. M.; Kim, Y.; Ko, Y. H.; Oh, D. H.; Kim, K. *Angew. Chem., Int. Ed.* **2007**, *46*, 7393−7395.
(28) Kim, K.; Selvapalam, N.; Ko, Y. H.; Park, K. M.; Kim, D.; Kim, J. *Chem. Soc. Rev.* **2007**, *36*, 267−279.

(29) Hwang, I.; Baek, K.; Jung, M.; Kim, Y.; Park, K. M.; Lee, D.-W.; Selvapalam, N.; Kim, K. *J. Am. Chem. Soc.* **2007**, *129*, 4170−4171.
(30) Lee, H.; Park, K.; Jeon, Y.; Kim, D.; Oh, D.; Kim, H.; Park, C.; Kim, K. *J. Am. Chem. Soc.* **2005**, *127*, 5006−5007.
(31) Huang, X.; Tan, Y.; Zhou, Q.; Wang, Y.; Che, Y. *Carbohydr. Polym.* **2008**, *74*, 685−690.
(32) Correia, H. D.; Demets, G. J.-F. *Electrochem. Commun.* **2009**, *11*, 1928−1931.
(33) Freeman, W.; Mock, W.; Shih, N. *J. Am. Chem. Soc.* **1981**, *103*, 7367−7368.
(34) Zhu, Y. J.; Tan, Y. B.; Du, X.; Piao, J. C.; Zhou, Q. F. *Chin. Chem. Lett.* **2008**, *19*, 355−358.
(35) Kim, K. US 7,388,099 B2 2008.
(36) Day, A. I.; Arnold, A. P.; Blanch, R. J. *Molecules* **2003**, *8*, 74−84.
(37) Ma, D.; Zavalij, P. Y.; Isaacs, L. *J. Org. Chem.* **2010**, *75*, 4786−4795.
(38) Lucas, D.; Minami, T.; Iannuzzi, G.; Cao, L.; Wittenberg, J. B.; Anzenbacher, P.; Isaacs, L. D. *J. Am. Chem. Soc.* **2011**, *133*, 17966−17976.
(39) Singh, G. S.; Pheko, T. *Spectrochim. Acta, Part A: Mol. Biomol. Spectrosc.* **2008**, *70*, 595−600.
(40) Tan, Y.; Choi, S.; Lee, J.; Ko, Y.; Kim, K. *Macromolecules* **2002**, *35*, 7161−7165.
(41) Chambon, P.; Blanazs, A.; Battaglia, G.; Armes, S. *Langmuir* **2011**, *28*, 1196−1205.
(42) Israelachvili, J. N. *Intermolecular and Surface Forces*; Academic Press: London: 2011.